Heliyon 10 (2024) e39333

Contents lists available at ScienceDirect

Heliyon

journal homepage: www.cell.com/heliyon

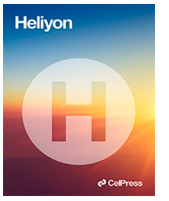

Research article

Role of HDAC3 in the epithelial-mesenchymal transition of retinal pigment epithelium cells: Implications for proliferative vitreoretinopathy

Weikang Zou [a,1], Chunling Huang [a,1], Yuting Chen [a], Jing Tang [a], Qiqi Li [a], Qi Fang [a], Yulin Ma [a], Wei Wu [b,**], Songfu Feng [a,*]

[a] Department of Ophthalmology, Southern Medical University, Zhujiang Hospital, Guangzhou, China
[b] Department of Ophthalmology, Guangzhou Red Cross Hospital of Jinan University, Guangzhou, China

ARTICLE INFO

Keywords:
Proliferative vitreoretinopathy
Epithelial-mesenchymal transiton
Retinal pigment epithelium
Histone deacetylase 3
MAZ
AKT pathway

ABSTRACT

Proliferative vitreoretinopathy(PVR) is a type of fibrotic eye disease with a poor clinical prognosis. Increasing evidence has shown that the primary pathological mechanism of PVR is the epithelial-mesenchymal transition(EMT) of retinal pigment epithelium(RPE) cells. Histone deacetylase 3(HDAC3) is a crucial enzyme involved in regulating the acetylation level of proteins. Several studies have reported associations between HDAC3 levels and EMT in various tumors; however, the specific effect of HDAC3 on PVR remains largely unknown. The current study found that HDAC3 was highly expressed in both human PVR membranes and experimental PVR. In vivo, silencing HDAC3 in RPE cells reduced their ability to develop experimental PVR through suppression of EMT. In vitro, inhibition of HDAC3 in RPE cells suppressed EGF-mediated cell proliferation, migration, and EMT. Additionally, overexpression of HDAC3 in RPE cells promoted cell proliferation, migration, and EMT. Mechanistically, the results of chromatin immunoprecipitation (ChIP) and luciferase assays revealed a direct binding of the transcription factor MAZ to the promoter region of HDAC3, thereby promoting its transcription. Furthermore, It was demonstrated that HDAC3 facilitated EMT by interacting with AKT and contributing to its deacetylation. In summary, our findings indicated the involvement of HDAC3 in the EMT of RPE cells, as well as its role in PVR through the regulation of the AKT pathway. These results suggested that targeting HDAC3 could be a potential strategy for preventing and treating PVR.

1. Introduction

Proliferative vitreoretinopathy(PVR) is a fibrotic ocular disease that can be a primary reason for the failure of rhegmatogenous retinal detachment repair. PVR occurs in around 5 %–10 % of all retinal detachment cases, and the clinical prognosis for patients with

* Corresponding author. Department of Ophthalmology, Southern Medical University, Zhujiang Hospital, No. 253, Gongye Avenue middle, Guangzhou, Guangdong, 510282, China.
** Corresponding author. Department of Ophthalmology, Guangzhou Red Cross Hospital of Jinan University, No.396 Tongfu Road, Guangzhou, Guangdong, 510000, China.
E-mail addresses: wuwei200414952@126.com (W. Wu), fsf516@163.com (S. Feng).
[1] Weikang Zou and Chunling Huang contributed equally to this project and should be co-first authors.

https://doi.org/10.1016/j.heliyon.2024.e39333
Received 5 March 2024; Received in revised form 11 October 2024; Accepted 11 October 2024
Available online 11 October 2024

PVR remains generally poor [1,2]. Surgery is presently the primary treatment for PVR, but it frequently recurs after the operation [1]. Despite advancements in vitreoretinal techniques, the incidence of PVR has not significantly changed [3]. Thus, a more comprehensive understanding of the pathogenesis of PVR is necessary to search for effective treatments for PVR.

PVR is defined by the expansion and contraction of the proliferative membranes on both sides of the retinal surface, which can contribute to tractional retinal detachment and severe vision loss [4]. The proliferative membranes within PVR consist of the extracellular matrix and various fibrous cellular components [5], with retinal pigment epithelium(RPE) cells being the principal cell type [6]. Recent studies have provided increasing evidence to support the notion that the epithelial-mesenchymal transition(EMT) of RPE cells is a crucial event in the formation of PVR [7,8]. During the EMT process, epithelial markers such as E-Cadherin are downregulated in RPE cells, whereas mesenchymal markers such as α-smooth muscle actin(α-SMA) and matrix metalloproteinase-9(MMP-9) are upregulated [9]. Following EMT, RPE cells lose their polarity and tight junctions, eventually transforming into myofibroblasts and contributing to the formation of proliferative membranes [10]; however, the specific regulatory mechanisms of this process are still unknown. Therefore, it is critical to investigate the molecular mechanisms of the EMT process in RPE cells along with the course of PVR to target RPE cells for the treatment of PVR.

Multiple studies reported that epigenetic changes, such as DNA methylation and mRNA methylation, were crucial in regulating the EMT of RPE cells [11,12]. However, recent studies have shown that histone acetylation also played a significant role in modulating various biological processes [13–15]. Histone deacetylases(HDACs) are important enzymes that modulate the acetylation level of proteins [16]. Among the HDACs family, HDAC3 is a critical and specific member, which is required for embryonic growth, development, and physiological function [17]. Recently, HDAC3 has been found to regulate the EMT of several epithelial cells in tumors and pulmonary fibrosis [16,18–20]. Nevertheless, it is still unknown whether HDAC3 is also involved in the EMT of RPE cells during PVR formation. To gain a deeper understanding of the regulatory mechanism of PVR, it is crucial to elucidate the role of HDAC3 in the EMT of RPE cells.

In this study, a mouse model of PVR and an EMT model of RPE cells were employed to test the potential effect of HDAC3 on PVR. The findings showed that inhibiting HDAC3 slowed the progression of PVR in vivo and suppressed the EMT process of RPE cells in vitro. Mechanistically, it was demonstrated that HDAC3 regulated the process of EMT by interacting with AKT. In summary, our findings highlighted the crucial role of HDAC3 in regulating PVR formation and EMT of RPE cells, and understanding this regulatory mechanism could offer new insights for preventing and treating PVR.

2. Materials and methods

2.1. PVR microarray profile collection and differentially expressed HDACs screening

The Gene Expression Omnibus(GEO) database, available at http://www.ncbi.nlm.nih.gov/geo, is an internet-based public repository for genome data, specifically high-throughput gene expression datasets. The gene expression profile GSE179603, obtained from the GEO database using the search terms 'proliferative vitreoretinopathy', was based on the GPL15433 platform. GSE179603 comprises ten human PVR membranes and ten macular puckers. All mRNA data for HDACs was downloaded for further analysis.

2.2. PVR induction in mice eyes

The study obtained approval from the medical ethics committee of Zhujiang Hospital of Southern Medical University for all animal experiments(LAEC-2021-145) and followed the guidelines of the Declaration of Helsinki. In short, male C57BL/6 mice aged 6–8 weeks and weighing 20±3g were purchased from the ZhuhaiBesTestBio-TechCo,Ltd. The mice were anesthetized using chloral hydrate, followed by the application of an antibiotic and a topical anesthetic to the right eye. Subsequently, the mice model of PVR was created by injecting 3 μL of human retinal pigment epithelial cell line(APRE-19, 1×10^6 per μL in PBS[pH 7.4]) into the vitreous cavity of the eyes using a 33G Hamilton syringe [21]. The control mice received the same volume of PBS(pH 7.4) injection. To inhibit HDAC3, the vitreous cavity was injected with ARPE-19 cells expressing low levels of HDAC3 (100 nM of siHDAC3). Additionally, control vector cells were injected into the PVR model mice in the control groups. After the operation, the right eye was coated with an antibiotic eye ointment. All mice were sacrificed using cervical dislocation at 14 days after the operation and the eyes were used for the subsequent experiments.

2.3. ARPE-19 cells culture and treatment

The ARPE-19 cells were purchased from Procell Technology Co., Ltd and were grown in Dulbecco's modified Eagle's medium (DMEM)/F12 medium(Gibco) with 10 % fetal bovine serum(FBS, Gibco) and 1 % penicillin-streptomycin(Hyclone) at 37 °C with 5 % CO_2. All of the experiments employed ARPE-19 cells at passages 4–6. Human recombinant EGF(MedChemExpress) was used at a concentration of 20 ng/ml to induce EMT in the ARPE-19 cells. The cells were treated with 15 μM of RGFP966(MedChemExpress) to suppress HDAC3 activity, as recommended by the manufacturer. To inhibit AKT signaling, the cells were treated with 10 μM of MK-2206(MedChemExpress). CHX(MedChemExpress) was used to block de novo protein synthesis at a concentration of 20 μM.

2.4. Protein-protein network construction

The protein network of HDAC3 related to EMT was created using STRING (https://cn.string-db.org/) with a medium confidence

score of 0.4. The network of protein-protein interactions among significantly associated proteins was constructed and displayed with the combined score.

2.5. Proliferation of APRE-19 cells

The growth of ARPE-19 cells was evaluated using the Cell Counting Kit-8(CCK-8, MedChemExpress) assay. Specifically, 4×10^3 ARPE-19 cells in 100 μL were placed in a 96-well plate. After treatment for 24 or 48 h, the cells were incubated with 90 μL of culture medium and 10 μL of CCK-8 solution at 37 °C for 2 h. The optical density was measured using a microplate reader at a wavelength of 450 nm. The proliferative capacity of ARPE-19 cells was quantified by subtracting the optical density of the blank wells from that of each well.

2.6. Migration of ARPE-19 cells

The movement of ARPE-19 cells was assessed using both the wounding healing and transwell assay. In the wounding healing assay, cells were initially cultured in 6-well plates until reaching 80 % density, at which point scratches were created using a 200 μL tip. Afterward, the old medium was taken out and substituted with a new fresh serum-free medium containing the test substance(EGF, RGFP966, MK-2206, or siHDAC3) or a control. The cells were then observed and imaged using an optical microscope at 0, 24, and 48h. The width of the scratch was determined by measuring the distance between its two edges with Image J software.

In the transwell assay, 4×10^4 cells in 200 μL of DMEM/F12 without FBS were placed in the upper chamber of an 8-μm pore transwell system(Corning Incorporated), while 700 μL of DMEM/F12 containing 10 % FBS was added to the lower chamber in a 24-well plate. The upper chamber was carefully submerged in the liquid of the lower chamber with sterile. The 24-well plate with transwell chamber was then placed in a 37 °C incubator for either 24 or 48 h. Following this incubation period, the liquid from the upper chamber was extracted and rinsed three times with 600 μL of PBS in a well. The cells remaining in the upper well were wiped away, while the cells that migrated onto the lower side were fixed with methanol for 30 min and then stained for another 30 min at room temperature with 0.1 % crystal violet(Bioss Biotechnology). A phase contrast microscope was used to observe the stained cells, and ImageJ was used to count the cells.

2.7. Real-Time PCR

The RNA extraction from ARPE-19 cells was carried out using the TRIzol reagent. Subsequently, an aliquot of 1 μg of total RNA was used to perform reverse transcription into cDNA using the SuperScript first-strand synthesis system. Quantitative PCR was conducted using the Power SYBRGreen PCR MasterMix, with the primer sequences detailed in Table 1.

2.8. Transfection with siRNA and plasmid

All siRNA and plasmids were obtained from IDT DNA Technologies. Transfection of plasmids and siRNA was performed using jetPRIME (Polyplus-transfection S.A) in accordance with the manufacturer's protocol. To transfect with siRNA, the cells underwent transient transfection with 5.5 μl of siHDAC3, siMAZ, or siNC, 50 μM in stock, mixed with 200 μl buffer and 4 μl reagent of jetPRIME. To transfect with the plasmid, the cells transfected with 1 μg of pcDNA3.4-HDAC3 (OE-HDAC3), pcDNA3.4-MAZ (OE-MAZ), or pcDNA3.4-NC (OE-NC), which mixed with 200 μl buffer and 2 μl reagent of jetPRIME. After transfecting for 48 h, the cells were prepared for individual experiments. The sequences of siRNA are shown in Table 2.

2.9. Histological and immunofluorescence detection

On day 14, all mice were sacrificed using cervical dislocation. The eyes were then incubated and fixed with 4 % paraformaldehyde for 24 h, followed by dehydration using reagent alcohol in a gradient. Subsequently, the dehydrated samples were fixed in paraffin and cut to a thickness of 4 μm. Masson's trichrome staining was conducted to analyze the histology of the retina, following a standard protocol by Masson Staining Kit(Solarbio Technology).

For the immunofluorescence analysis, tissue slices were fixed in fresh 4 % paraformaldehyde for 15 min and then washed three times with PBS, each wash lasting 5 min. The fixed cells were incubated with 5 % bovine serum albumin (BSA) for 1 h at room temperature, followed by overnight incubation at 4 °C with HDAC3 (1:200, Abcam) or alpha-SMA (1:200, Abcam) antibodies. After three additional washes with PBS, the samples were incubated for 1 h at room temperature with a Dylight 594 fluorescent-labeled goat anti-rabbit secondary antibody, followed by 15 min of staining with 4′,6-diamidino-2-phenylindole (DAPI). The images were then

Table 1
Primer sequences used in Real-Time PCR.

Primers	Forward primer	Reverse primer
HDAC3	CCACTCCGAGGACTACATTGACTTC	CGTTGACATAGCAGAAGCCAGAGG
MAZ	GAGCAGGAGGAAGAGCCAGGAG	GGACACAGGAACACGATGACATGG
β-actin	TGCTGTCCCTGTATGCCTCTGG	ACCGCTCGTTGCCAATAGTGATG

Table 2
The sequences of siRNA used in transfection.

siRNA	sequences
siHDAC3	CUGACAAUGGUACCUAUUATT
siMAZ	CCAAGUUGGUUGCGGGGGATT
siNC	UUCUCCGAACGUGUCACGUTT

captured using a Nikon microscope.

2.10. Western blotting and immunoprecipitation(IP)

Protein was isolated from mice retinal samples and ARPE-19 cells, and the concentration was measured using a Pierce BCA Protein Assay Kit(KeyGEN). After being separated using sodium dodecyl sulfate-polyacrylamide gel electrophoresis (SDS-PAGE) with 20 μg of proteins per sample, the proteins were transferred onto polyvinylidene difluoride(PVDF, Merck-Millipore) membranes. Following electro-blotting onto PVDF membranes, 5 % BSA was used to block the membranes for a full hour at room temperature. Subsequently, the membranes were incubated at 4 °C overnight with primary antibodies, including HDAC3(1:1000, Affinity), alpha-SMA(1:1000, Affinity), E-cadherin (1:1000, Proteintech), MMP-9(1:1000, Bioss Biotechnology), MAZ(1:1000, Affinity), acetylated-lysine(1:1000, Abmart), ubiquitin(1:500, HuaBio), AKT(1:1000, Zen-Bioscience), phospho-AKT(1:1000, Zen-Bioscience), and glyceraldehyde 3-phophate dehydrogenase(GAPDH, 1:1000, Fude Biotechnology). The membranes were then rinsed three times with 0.1 % TBST before incubating with secondary antibodies for an hour at room temperature. Finally, the protein bands were visualized using an ECL-plus Western blotting detection system, and ImageJ was used for analysis. The expression of GAPDH served as an internal control.

The IP was carried out following a standard protocol by IP Kit(Thermo Fisher Scientific). In brief, the antibodies stock including HDAC3(HuaBio), AKT(HuaBio), and negative control IgG was diluted with IP lysis buffer to achieve a final concentration of 5μg/100 μL. The lysates of APRE-19 cells were isolated using an IP lysis buffer. Depending on the protein concentration measured, the total protein was adjusted to 500 μg, and then the cell lysates were diluted to 500 μL with IP lysis buffer. Subsequently, the 500 μL of diluted cell lysates were incubated with the 100 μL of diluted antibodies overnight at 4 °C in a tube. Each tube received 30 μL of beads and was incubated at room temperature for an hour, with mixing. After combining with beads, the complex was washed in IP buffer three times before boiling with SDS buffer, which was then subjected to elution and western blotting.

2.11. Chromatin immunoprecipitation(ChIP) assay

ChIP was conducted using a Pierce Magnetic ChIP kit from Thermo Fisher Scientific. In the experiment, 1×10^7 cells were utilized, and MNase digestion was performed to break the crosslinked chromatin into 150- to 1000-bp pieces. Subsequently, the chromatin underwent immunoprecipitation using either 2 μg of rabbit IgG or 2 μg of rabbit anti-MAZ antibody, which were rotated overnight at 4 °C. After adding 20 μL of magnetic beads to each tube, the tubes were mixed and incubated at 4 °C for 2 h. The magnetic beads were then subjected to five washes with IP wash buffer and subsequently eluted. qRT-PCR was used to examine the immunoprecipitated chromatin following purification. Primers used in PCR were designed within the promoter region(Table 3).

2.12. Luciferase assay

The cells (4 × 104) were seeded in 24-well plates and cultured for 24h for a dual-luciferase reporter gene assay. Luciferase was linked to HDAC3 wild-type (HDAC3 WT-Luc), HDAC3 Mut 1 (HDAC3 Mut 1-Luc), HDAC3 Mut 2 (HDAC3 Mut 2-Luc), or HDAC3 Mut 3 (HDAC3 Mut 3-Luc) reporter vector, respectively, then transfected into APRE-19 cells. After transfection, a Dual-Lcuiferase Reporter Assay Kit (Promega) was applied through the manufacturer's recommendations. 20 μL collected cell lysate of groups was added to a black label plate. A firefly luciferase reaction fluid was added and mixed, followed by detecting the activity of firefly luciferase within 30 min at 550 nm. A Renilla luciferase reaction fluid was then added to each well and mixed, followed by detecting the activity of Renilla luciferase within 30 min at 480 nm.

2.13. Statistical analysis

The data were represented as the mean ± SD. Statistical analyses were conducted using Prism 8.0(GraphPad) based on the results of three separate experiments. The differences between groups were compared using the student's *t*-test or one-way analysis of variance

Table 3
Primer sequences used in Chromatin immunoprecipitation (ChIP).

Primers	Forward primer	Reverse primer
Primer1	TTTGGCCTGGGTCTGTTGGT	AGACGTGCTTGTTTCAGATCCTG
Primer2	CACGAGATGGGACGGCATTCTTAG	GGGAGGGGAGGAATCAAGGGATG
Primer3	ATACCCGCGCCGTGGCA	ATAGACCAGTGGACAACACCCACG

(ANOVA). Statistical significance was determined using *$P < 0.05$, **$P < 0.01$, ***$P < 0.001$ and ****$P < 0.0001$.

3. Results

3.1. HDAC3 was overexpressed in human PVR membranes

All original data from GSE179603 were uploaded to Sangerbox (http://www.sangerbox.com/tool) for the assessment of differentially expressed HDACs, using the criterion of a p value < 0.05 and a Fold Change>1.2. The expressed HDACs mRNA of the data set was visualized through heat maps in Fig. 1A. Among these HDACs, HDAC3 exhibited the highest expression abundance and was identified as one of the most upregulated HDACs, thus warranting further investigation(Fig. 1B). Fibronectin1(FN1), alpha-1 type I collagen(COL1A1), alpha-2 type II collagen(COL1A2), and alpha-1 type III collagen(COL3A1) were the main fibrotic components of PVR membranes and increased in PVR(Fig. 1C). Notably, these four proteins demonstrated a significant correlation in expression with HDAC3, as indicated by the intensity reads from the microarray data(Fig. 1D, E, F, and G).

3.2. Downregulation of HDAC3 inhibited the progression of the PVR mice model

To confirm our findings, we established the PVR mice model by injecting ARPE-19 cells intravitreously. The masson's trichrome staining showed that the epiretinal membrane attached to the inner retinal layer, followed by the alterations in the retina structure and detachment of the retina in the PVR mouse model(Fig. 2A). Western blot analysis validated an elevated production of HDAC3 in the retinal tissues of the PVR mouse model(Fig. 2B). The results of immunofluorescence further demonstrated an increased expression of HDAC3 in the proliferative membrane of the PVR mouse model(Fig. 2C). To evaluate the effect of HDAC3 on the PVR mice model, the vitreous cavities of mice were injected with PBS, cell suspension of the siNC, or the siHDAC3, respectively. Our findings indicated that the disruption in the retina was mitigated in the PVR + siHDAC3 group, as opposed to the PVR + siNC group, where the retinal

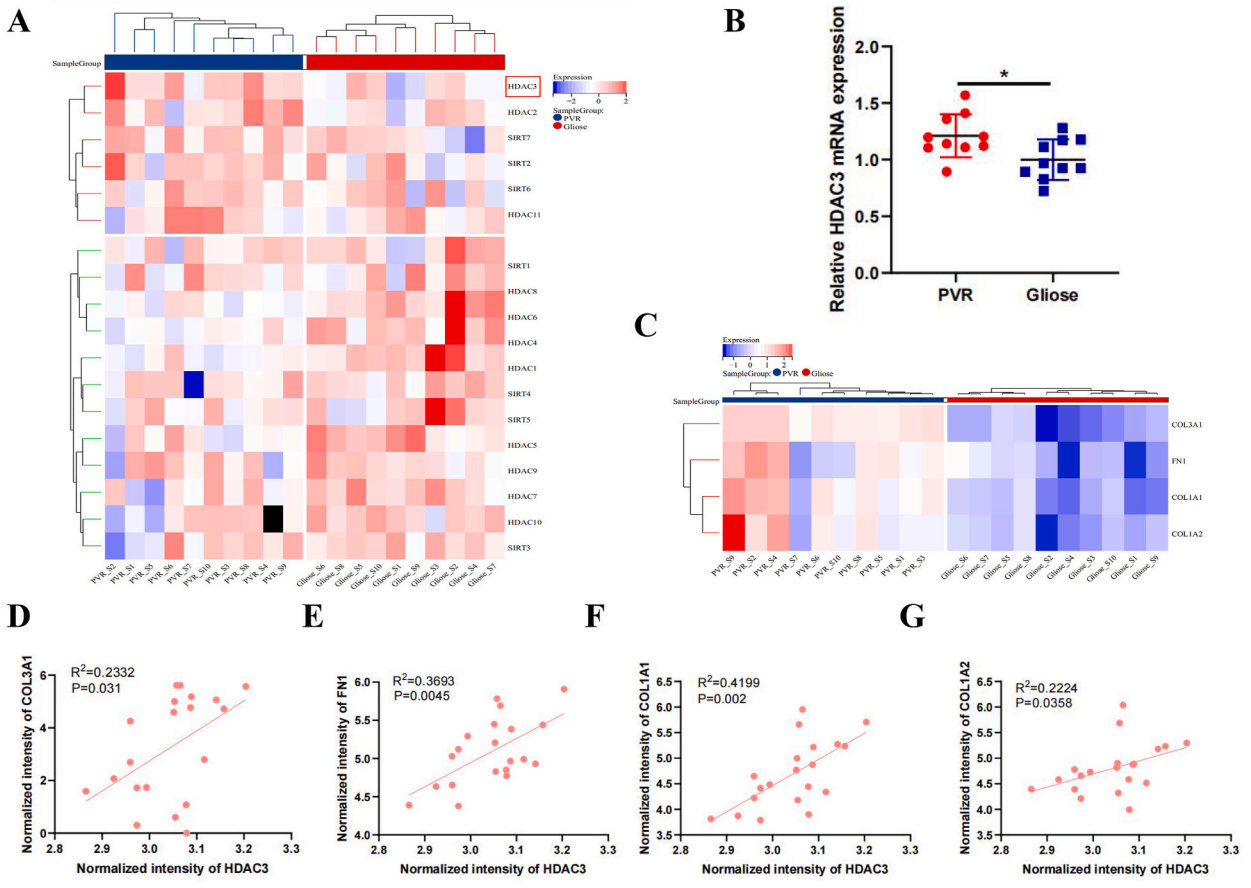

Fig. 1. HDAC3 was up-regulated in human PVR membranes. (A)Heat map of HDACs expression in GSE179603 data set. (B)The HDAC3 mRNA expression between human PVR membranes and macular pucker. *P < 0.05; n = 10. (C)Heat map of FN1, COL1A1, COL1A2 and COL3A1. (D)The expression relationship of HDAC3 and COL3A1 in GSE179603. (E)The expression relationship of HDAC3 and FN1 in GSE179603. (F)The expression relationship of HDAC3 and COL1A1 in GSE179603. (G)The expression relationship of HDAC3 and COL1A2 in GSE179603.

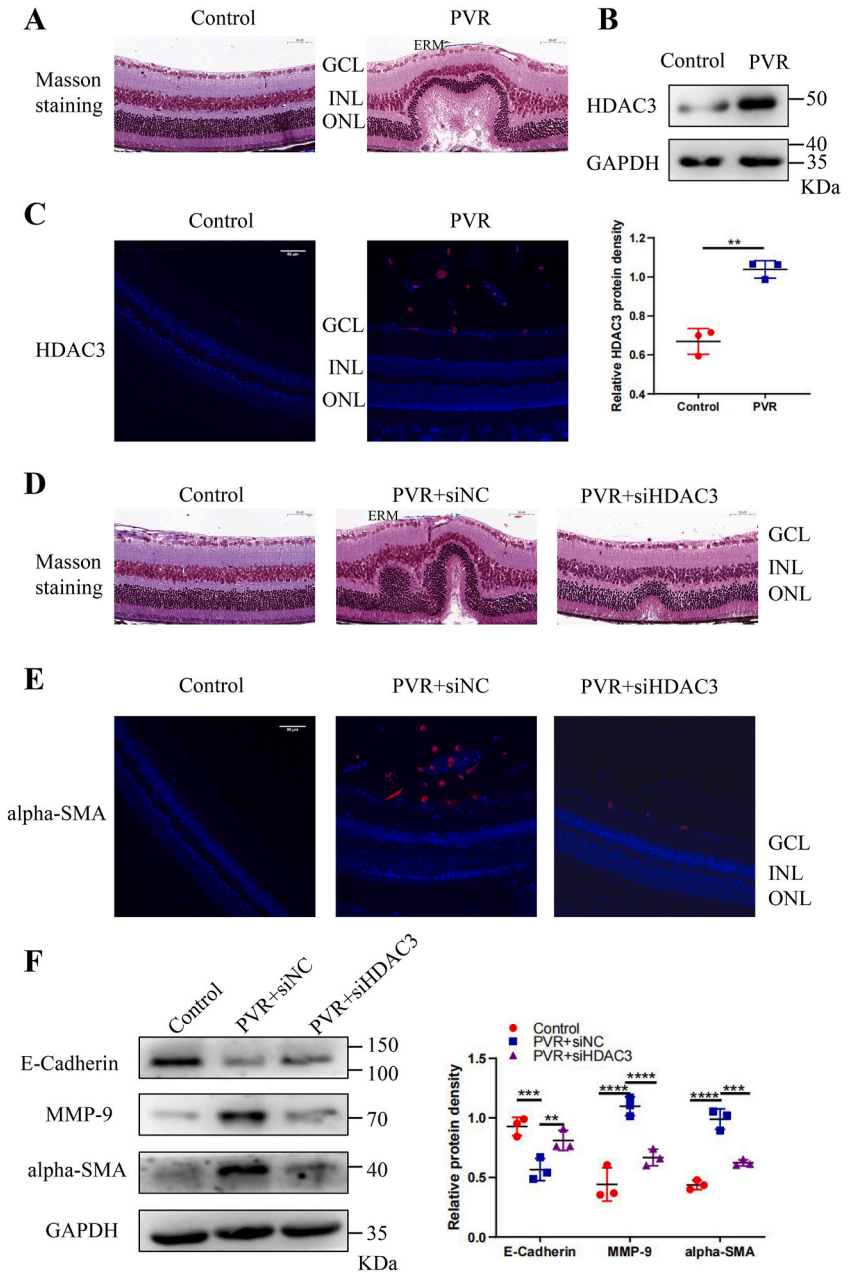

Fig. 2. Downregulation of HDAC3 inhibited the progression of the PVR mice model. (A)Masson staining was performed on the retinas of mice to assess the proliferative membrane formation. Scale bar, 50 μm. n = 3. (B)The expression of HDAC3 in the retinal tissue of mice was detected by Western blot. ***$P < 0.001$; n = 3. (C)Immunofluorescence analysis was used to detect the expression of HDAC3. Scale bar, 50 μm. n = 3. (D)Masson staining in the retinal tissue of mice. Scale bar, 50 μm. n = 3. (E)The Immunofluorescence of alpha-SMA in the retinal tissue of mice. Scale bar, 50 μm. n = 3. (F)Western blot assay was conducted to assess the levels of E-Cadherin, MMP-9, and alpha-SMA expression in the retinal tissue of mice. *$P < 0.05$; **$P < 0.01$; ****$P < 0.0001$; n = 3.

structure was disrupted(Fig. 2D). Additionally, the expression of alpha-SMA, a myofibroblast marker [22,23], was lower in the PVR + siHDAC3 compared to the PVR + siNC group(Fig. 2E). According to Western blot analysis, alpha-SMA and MMP-9, two mesenchymal indicators, were downregulated in the PVR + siHDAC3 group, but the epithelial marker E-Cadherin was upregulated(Fig. 2F). These results indicated that the downregulation of HDAC3 could inhibit the progression of PVR by suppressing EMT in vivo.

3.3. HDAC3 was increased in ARPE-19 cells treated with EGF rather than TGFβ

Both transforming growth factor-beta(TGFβ) and epidermal growth factor(EGF) were significantly upregulated with the vitreous in

PVR patients and often used to induce the EMT process in vitro [24,25]. In our study, we found that HDAC3 was upregulated in ARPE-19 cells treated with EGF rather than TGFβ1(Fig. 3A and B). Furthermore, treatment with different concentrations of EGF induced a gradual increase in HDAC3 at the mRNA and protein level(Fig. 3C and D). Meanwhile, HDAC3 expression also increased in ARPE-19 cells treated with 20 ng/ml EGF from 24 h to 48 h(Fig. 3E and F). These findings revealed that the upregulation of HDAC3 was mediated by EGF rather than TGFβ during the EMT process.

3.4. Inhibition of HDAC3 attenuated EGF-mediated cell proliferation, migration and EMT

To investigate the potential involvement of HDAC3 in the EGF-induced cells EMT model, ARPE-19 cells were treated with the HDAC3 inhibitor RGFP966 at a concentration of 15 μM. In the transwell assay, the migration rate of cells treated with the RGFP966 was notably reduced compared with the DMSO group at 24 h and 48 h in the existence of EGF(Fig. 4A and B). Consistent with the transwell assay, RGFP966 markedly decreased the rate of wound closure after 24 h and 48 h of EMT induction(Fig. 4C and D), indicating its ability to attenuate the migratory capacity of RPE cells during the EMT process. Additionally, the CCK-8 assay

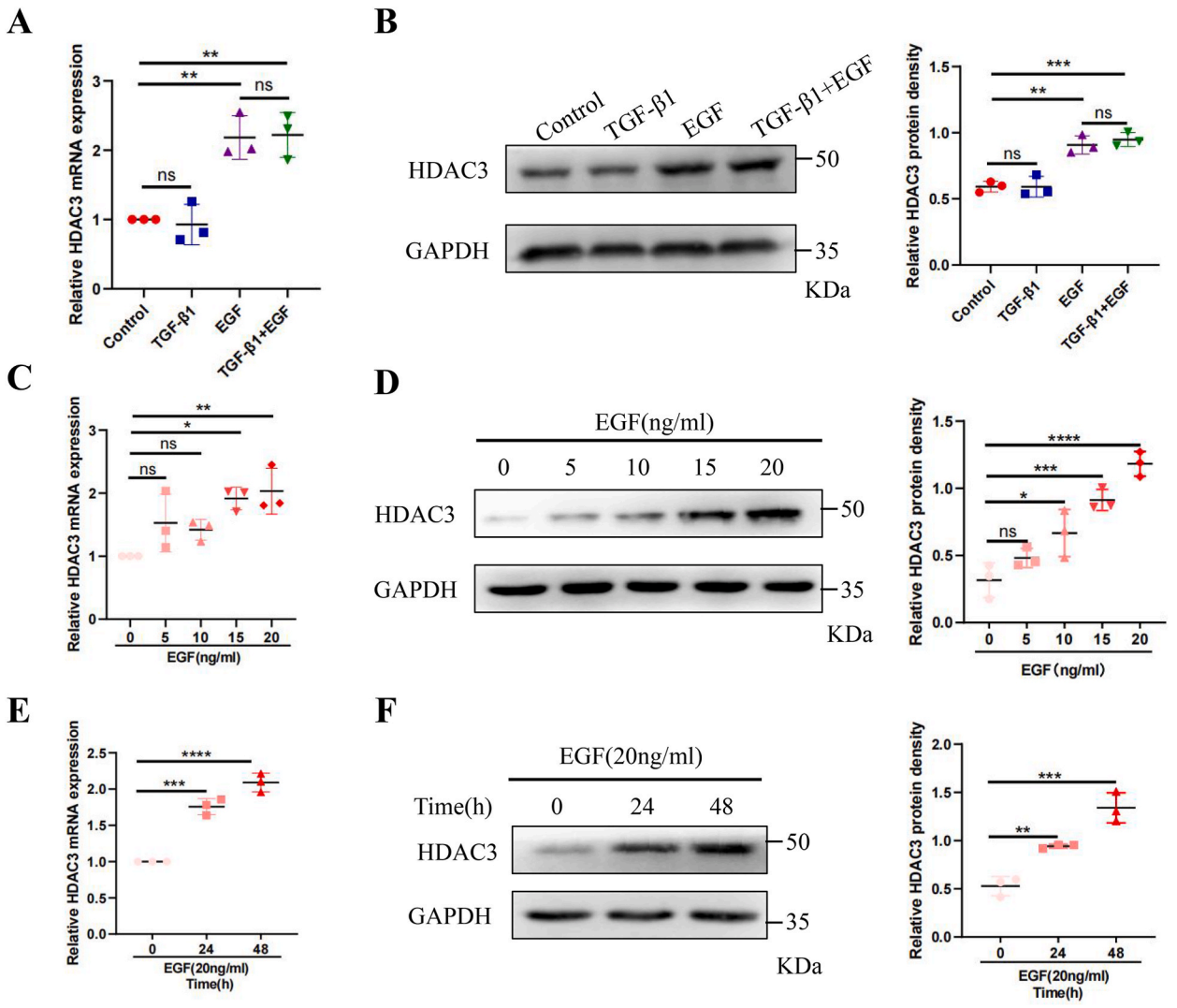

Fig. 3. HDAC3 was upregulated in EGF-induced EMT of ARPE-19 cells. (A)The Real-Time PCR was used to measure the mRNA expression of HDAC3 in ARPE-19 cells following treatment with TGFβ1 or EGF for 48 h $^{**}P < 0.01$; n = 3. (B)Western blot assay was conducted to assess the levels of HDAC3 expression in ARPE-19 cells following treatment with TGFβ1 or EGF for 48 h $^{**}P < 0.01$; $^{***}P < 0.001$; n = 3. (C)Real-Time PCR was used to determine the expression of HDAC3 in ARPE-19 cells following treatment with various doses of EGF(0, 5, 10, 15, and 20 ng/ml) for 48 h $^{*}P < 0.05$; $^{**}P < 0.01$; n = 3. (D)Western blot analysis for HDAC3 expression in ARPE-19 cells treated with various doses of EGF(0, 5, 10, 15, and 20 ng/ml) for 48 h $^{*}P < 0.05$; $^{***}P < 0.001$; $^{****}P < 0.000$; n = 3. (E)The Real-Time PCR was used to measure the mRNA level of HDAC3 in ARPE-19 cells following treatment with 20 ng/ml EGF at various periods. $^{***}P < 0.001$; $^{****}P < 0.000$; n = 3. (F)The protein level of HDAC3 in ARPE-19 cells was assessed using Western blot after treatment with 20 ng/ml EGF at various periods. $^{**}P < 0.01$; $^{***}P < 0.001$; n = 3.

demonstrated that RGFP966 significantly suppressed the EGF-induced cell proliferation following 24 h and 48 h(Fig. 4E). Furthermore, as shown in Fig. 4F, EGF induced a significant drop in the epithelial marker E-Cadherin and a rise in the mesenchymal indicators alpha-SMA and MMP-9, however, these changes at the protein level were prevented by RGFP966 treatment(Fig. 4F).

To further validate the involvement of HDAC3 in RPE cells EMT, HDAC3-siRNA was used to knock down the HDAC3 protein. A non-targeting siRNA was utilized as the control group. The HDAC3-siRNA greatly reduced the expression of their respective mRNA and protein(Fig. 5A). Notably, the suppression of HDAC3 resulted in a reduction in cell proliferation in response to EGF at both 24 and 48 h (Fig. 5B). As shown in Fig. 5C and D, in the wound healing assay, 20 ng/ml EGF enhanced the migration of APRE-19 cells, but this effect was significantly attenuated by HDAC3-siRNA. In the transwell system, the quantity of migrated cells was elevated under EGF treatment, but such an increase was diminished by HDAC3-siRNA (Fig. 5E and F). Furthermore, as illustrated in Fig. 5G, HDAC3 knockdown led to an increase in the expression of E-Cadherin and a decrease in the expression of alpha-SMA and MMP-9 (Fig. 5G). These findings suggested that HDAC3 was essential for EGF-induced EMT of RPE cells.

3.5. *Overexpression of HDAC3 promoted cell proliferation, migration, and EMT*

To further investigate the potential involvement of HDAC3 in the EMT of RPE cells, ARPE-19 cells were transfected with pcDNA3.4-HDAC3 to overexpress HDAC3 (OE-HDAC3). In the CCK-8 assay, the data showed that HDAC3 overexpression significantly enhanced cell proliferation following 24 h and 48 h (Fig. S1A). As shown in the wound healing assay, HDAC3 overexpression increased the rate of

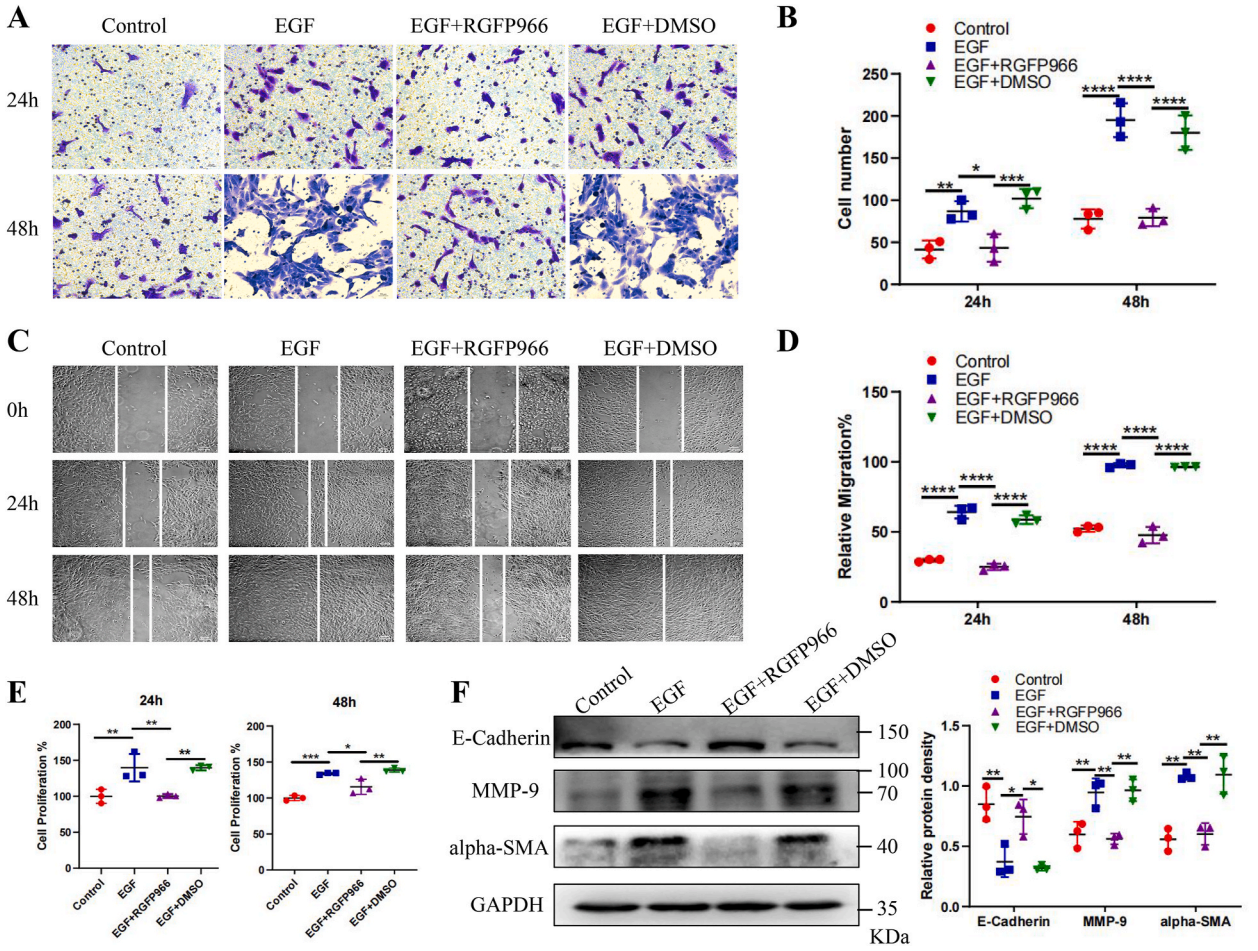

Fig. 4. RGFP966 suppressed the cell proliferation, migration, and EMT induced by EGF in ARPE-19 cells. (A)The transwell assay was used to detect the migration of ARPE-19 cells treated with 20 ng/ml EGF and 15 μM RGFP966 for 24 h and 48 h. Scale bar, 25 μm. n = 3. (B)Statistical analysis of the quantity of cells that migrated through the upper chamber. *$P < 0.05$; **$P < 0.001$; ***$P < 0.001$; ****$P < 0.0001$; n = 3. (C)The scratch assay was used to examine ARPE-19 cells' wound-repair abilities. Scale bar, 100 μm. n = 3. (D)The quantitative assessment of the rate of wound closure. ****$P < 0.0001$; n = 3. (E)ARPE-19 cells were exposed to a combination of 20 ng/ml EGF and 15 μM RGFP966 for 24 h or 48 h. Cell proliferation was evaluated using the CCK-8 assay. *$P < 0.05$; **$P < 0.01$; ***$P < 0.001$; n = 3. (F)Western blot assay was conducted to analyze the levels of E-Cadherin, MMP-9, and alpha-SMA expression in APRE-19 cells treatment with RGFP966 or DMSO and exposure to EGF. *$P < 0.05$; **$P < 0.01$; n = 3.

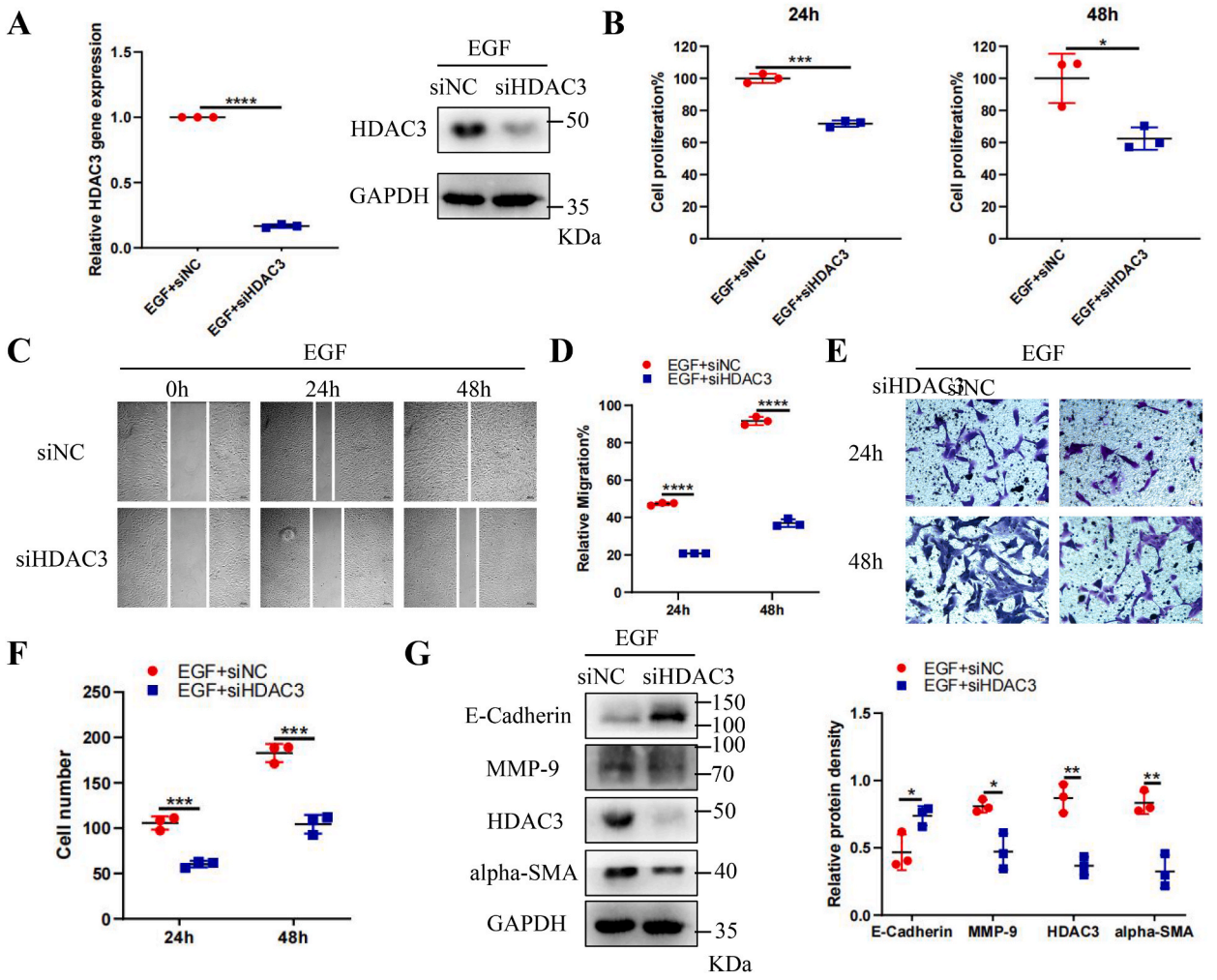

Fig. 5. HDAC3 knockdown inhibited the cell proliferation, migration, and EMT induced by EGF in ARPE-19 cells. (A)The expression of HDAC3 was detected using Real-Time PCR and Western blot after transfecting with siHDAC3 or siNC in ARPE-19 cells. ****$P < 0.0001$; n = 3. (B) The cell proliferation was examined using CCK-8 assay after transfecting with siHDAC3 or siNC in ARPE-19 cells. *$P < 0.05$; ***$P < 0.001$; n = 3. (C) ARPE-19 cells that were transfected with siHDAC3 or siNC were subjected to the examination of cell migration using the scratch assay. Scale bar, 100 μm. n = 3. (D)The statistical analysis of the data presented in Fig. 5C demonstrated the significant decrease in EGF-induced cell migration following the transfection of HDAC3-siRNA at both 24 and 48-h time points. ****$P < 0.0001$; n = 3. (E)The transwell assay was utilized to detect the migration of ARPE-19 cells that were transfected with siHDAC3 or siNC. Scale bar, 25 μm. n = 3. (F)The statistical analysis of the data presented in Fig. 5E revealed a significant decrease in EGF-induced cell migration following the transfection of HDAC3-siRNA at both 24 and 48-h time points. ***$P < 0.001$; n = 3. (G)Western blot assay was conducted to analyze the levels of E-Cadherin, MMP-9, and alpha-SMA expression in APRE-19 cells transfected with siHDAC3 or siNC and exposure to EGF. *$P < 0.05$; **$P < 0.01$; n = 3.

wound closure after 24 h and 48 h (Fig. S1B). Consistent with the wound healing assay, the migration rate of cell transfection with the OE-HDAC3 was notably upregulated compared with the OE-NC group at 24 h and 48 h (Fig. S1C), indicating its ability to promote the migratory capacity of RPE cells. Additionally, the Western blot assay demonstrated that the epithelial marker E-Cadherin was decreased, while the mesenchymal indicators alpha-SMA and MMP-9 were increased in the HDAC3 overexpression group (Fig. S1D). These data demonstrated that HDAC3 was essential in the EMT process of RPE cells.

3.6. The transcription factor MAZ bound directly to the promoter region of HDAC3 and promoted its expression

The study delved into the regulatory mechanisms of the expression of HDAC3 in RPE cells treated with EGF. Potential transcription factors that could bind to the promoter region of HDAC3 were predicted using the PROMO tool (http://alggen.lsi.upc.es/cgi-bin/promo_v3/promo/promoinit.cgi?dirDB=TF_8.3)(Fig. 6A). Among these transcription factors, three(MAZ, AHR, and RAR-alpha) showed significant differences in expression in human PVR membranes based on the microarray results(Fig. 6B). Of these, MAZ, a Myc-associated zinc-finger protein known to bind to a GA box(GGGGAGGG)(Fig. 6C), exhibited a significant correlation in expression

with HDAC3 based on the microarray data intensity reads (Fig. 6D). This correlation was further confirmed through western blotting of MAZ and HDAC3 in ARPE-19 cells treated with or without EGF, and their expression relationship was compared using linear regression. Similarly, both MAZ and HDAC3 showed significant increases in ARPE-19 cells treated with EGF, and a significant link was found between these two genes(Fig. 6E and F). Additionally, we investigated a 2 kb region upstream of HDAC3's transcription start site using the PROMO online toll, and three MAZ-binding motifs from −1315 to −1033, −889 to −874, and −822 to −807 were identified (Fig. 6G). Subsequently, ChIP assays were conducted to determine whether MAZ directly was bound to the promoter region of HDAC3. Three primer pairs were designed based on the potential binding sites within the 2000 bp upstream of HDAC3(Fig. 6H), and qRT-PCR with the ChIP product and three primer pairs indicated that MAZ was enriched at the three HDAC3 promoter sites(Fig. 6I). Luciferase assays were also performed to identify the regions of HDAC3 that might be bound by MAZ. As shown in Fig. S2, the luciferase reporter activity of HDAC3 was upregulated by co-transfection with the MAZ-overexpression plasmid (OE-MAZ) in ARPE-19 cells in HDAC3-WT group, as well as HDAC3-Mut 1 and HDAC3-Mut 2 group, while the luciferase reporter activity of HDAC3 was no significant difference in HDAC3-Mut 3 group compared with the pcDNA3.4-NC control vectors (OE-NC) (Fig. S2). To further determine the relationship between MAZ and HDAC3, a specific siRNA targeting MAZ was synthesized and transfected into ARPE-19 cells treated with EGF. The siMAZ inhibited the EGF-induced expression of MAZ, and the knockdown of MAZ inhibited the EGF-mediated upregulation of HDAC3(Fig. 6J and K).

3.7. HDAC3 mediated APRE-19 cells EMT by regulating AKT phosphorylation

To determine the specific signaling pathways associated with HDAC3, a protein-protein interaction(PPI) network involving HDAC3 and EMT-related signaling was established using data from the STRING database(https://cn.string-db.org). The analysis revealed that the top three significant EMT-related signaling pathways linked to HDAC3 were TNF(0.921), AKT1(0.666), and STAT1(0.407), based on a combined score of each interaction with a confidence level of 0.4. Given that the interaction between HDAC3 and TNF has been previously examined and the regulation of AKT by HDAC3 has not been fully explored [26–28], the relationship between HDAC3 and AKT was investigated. In vivo, we found that the phosphorylation of AKT was downregulated in the PVR + siHDAC3 group(Fig. 7B). To further clarify the cross-talk signaling between HDAC3 and AKT, the EGF-mediated AKT phosphorylation was tested after treatment with RGFP966 or transfected with siHDAC3. The results indicated that the inhibition of HDAC3 reduced the EGF-evoked AKT phosphorylation in ARPE-19 cells(Fig. 7C and D), suggesting that HDAC3 played a pivotal role in regulating AKT phosphorylation.

The AKT pathway plays a crucial role in EGF-induced EMT of ARPE-19 cells. We also investigated the role of the AKT pathway in EGF-induced EMT in PRE cells. Transwell assay indicated that AKT inhibitor MK-2206 of 10 μM inhibited ARPE-19 cell migration in response to EGF(Fig. 8A and B). Consistent with the transwell assay, the wound healing assay showed that MK-2206 suppressed EGF-induced cell migration (Fig. 8C and D). Additionally, treatment with MK-2206 also reduced EGF-mediated cell growth(Fig. 8E). Furthermore, Western blot analysis showed that the mesenchymal markers alpha-SMA and MMP-9 were downregulated in the EGF + MK-2206 group, whereas the epithelial marker E-Cadherin was upregulated in comparison to the EGF group(Fig. 8F). These results confirmed that HDAC3 was involved in EGF-induced EMT of RPE cells by regulated AKT pathway signaling.

3.8. HDAC3 promoted the phosphorylation of AKT by deacetylating AKT

To further clarify whether AKT phosphorylation regulated by HDAC3 was attributed to its potential regulation of the expression of upstream regulators, and thus indirectly impacting AKT phosphorylation, ARPE-19 cells were subjected to cycloheximide(CHX) treatment to impede de novo protein synthesis. Surprisingly, the CHX treatment had only a minimal impact on RGFP966-induced suppression of AKT phosphorylation (Fig. 9A), implying that RGFP966's lowered AKT phosphorylation was not largely mediated by its effect on the expression of AKT upstream regulators.

It was reported that Polyubiquitination plays a critical role in the phosphorylation of AKT [29]. Our study revealed that the polyubiquitination of AKT increased in ARPE-19 cells following EGF treatment, and this effect was time-dependent(Fig. 9B). Considering the potential competition between acetylation and polyubiquitination at the same lysine residues [30], we examined the regulatory role of HDAC3 in AKT acetylation. Initially, we indicated the interaction between HDAC3 and AKT in ARPE-19 cells (Fig. 9C). Then, we found that inhibition of HDAC3 by RGFP966 or siRNA increased AKT acetylation(Fig. 9D and E), but decreased AKT polyubiquitination and phosphorylation(Fig. 9F and G). These results suggested that HDAC promoted the phosphorylation of AKT by deacetylating AKT.

4. Discussion

The EMT of RPE cells is a critical pathological mechanism in the development of PVR, which ultimately contributes to the formation of proliferative membranes and results in substantial impairment of vision [1,31,32]. Focusing on RPE cells may represent a promising therapeutic approach for preventing and treating PVR. Currently, the potential regulatory mechanism of RPE-EMT remains largely unknown. In the present investigation, we have demonstrated that the upregulation of HDAC3 expression occurred in mice with PVR induced by intravitreal injection of RPE cells and EGF-induced RPE cell EMT. In vivo, knockdown HDAC3 in RPE cells resulted in the inhibition of the experimental PVR progression through suppression of EMT. In vitro, it was observed that HDAC3 inhibition attenuated cell proliferation, migration, and the expression of EMT markers. Furthermore, HDAC3 overexpression promoted cell proliferation, migration, and EMT in RPE cells. Mechanistically, HDAC3 enhanced the phosphorylation levels of AKT by binding to AKT and promoting its deacetylation. The data of the current study support the hypothesis that HDAC3 is significantly involved in the EMT of

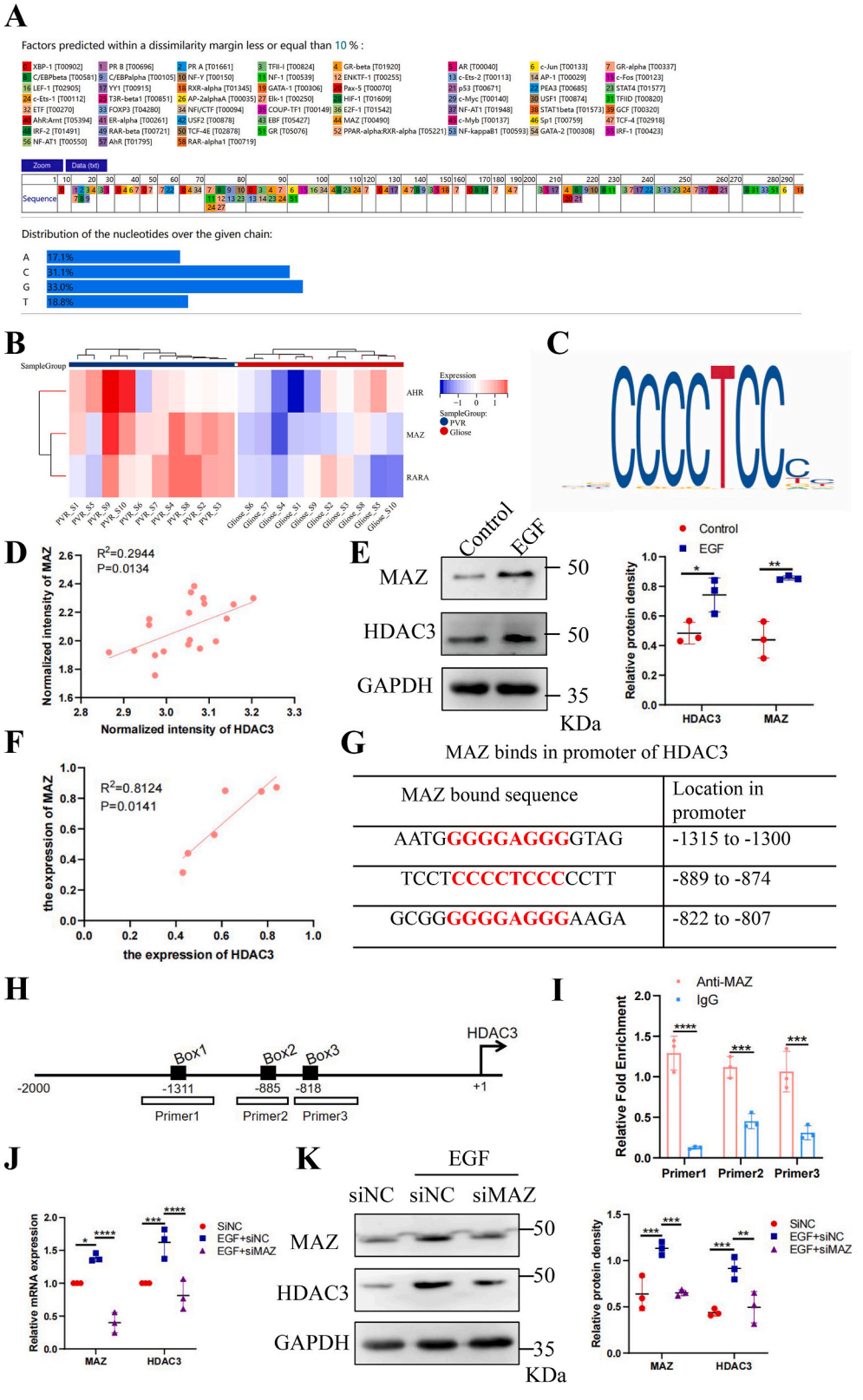

(caption on next page)

Fig. 6. Direct binding of the transcription factor MAZ to the HDAC3 promoter region increased the expression of HDAC3. (A)Transcription factors that may have been bound to the promoter region of HDAC3. (B)Heat maps of AHR, MAZ, and RAR-alpha expression in GSE179603 data set. (C)The sequence was directly bound by MAZ. (D)The correlation between HDAC3 and MAZ was determined by analyzing the intensity reads obtained from the microarray data. n = 10. (E)The levels of HDAC3 and MAZ were assessed in ARPE-19 cells following treatment with or without EGF using Western blot analysis. $*P < 0.05$; $**P < 0.01$; n = 3. (F)The relationship between HDAC3 and MAZ expression in ARPE-19 cells following treatment with or without EGF. n = 6. (G)MAZ may have been linked to the promoter region of HDAC3 within a 2 kb region. (H)The three primers were based on the three potential sites within the 2000 bp upstream of HDAC3. (I)ChIP assays were conducted to investigate the direct binding of MAZ to the promoter region of HDAC3. $***P < 0.001$; $****P < 0.0001$; n = 3. (J) The levels of MAZ and HDAC3 were assessed using Real-Time PCR after transfecting with siMAZ and exposure to EGF. $*P < 0.05$; $***P < 0.001$; $****P < 0.0001$; n = 3. (K)The levels of MAZ and HDAC3 were measured using Western blot analysis after transfecting with siMAZ and exposure to EGF. $**P < 0.01$; $***P < 0.001$; n = 3.

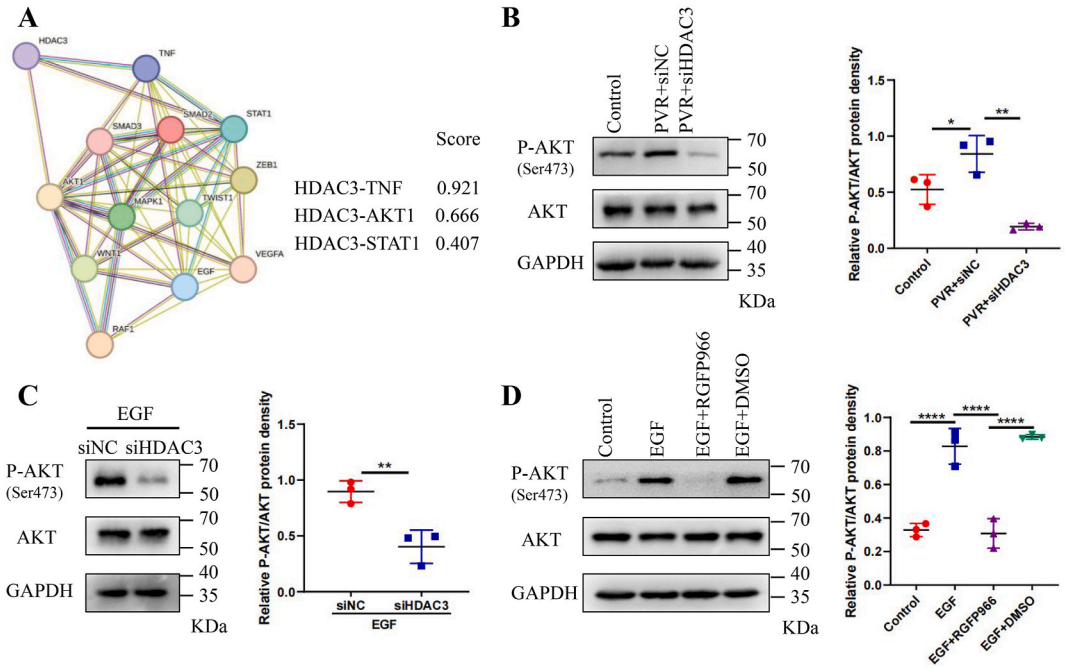

Fig. 7. The activation of AKT in PVR was reliant on the activation of HDAC3. (A)A PPI network involving HDAC3 and signaling pathways related to EMT was established using data sourced from the STRING database. (B)Western blot analysis was conducted to assess the levels of AKT and phospho-AKT expression in the mice's retinal tissue. $*P < 0.05$; $**P < 0.01$; n = 3. (C)Western blot analysis was conducted to assess the levels of AKT and phospho-AKT expression in APRE-19 cells that were transfected with siHDAC3 or siNC and exposed to EGF. $****P < 0.0001$; n = 3. (D) Western blot analysis was conducted to assess the levels of AKT and phospho-AKT expression in APRE-19 cells treated with RGFP966 or DMSO and exposed to EGF. $**P < 0.01$; n = 3.

RPE cells during the progression of PVR, which may be regarded as a potential target for PVR.

HDAC3 is a particular member of the class I HDACs, which also include HDAC1, HDAC2, and HDAC8 [16]. Previous reports have shown that HDAC3 was different compared with HDAC1 and HDAC2 in that HDAC3 had an intriguingly variable C terminus [18,33], indicating that HDAC3 may have several unique functions in various physiological and pathological events such as EMT. A recent study showed that HDAC3 exacerbated EMT in alveolar type 2 epithelial cells(AT2) and contributed to the development of pulmonary fibrosis by deacetylating GATA3 and impeding its degradation [19]. Furthermore, it was reported that HDAC3 could have a significant impact on the process of EMT in a variety of cancer cell types, including those found in gastric and breast cancer [18,34]. In addition, the link between HDACs and RPE-EMT has been revealed in a previous study, which found that some of class I and class II were increased in RPE cells stimulated with TGFβ, excluding HDAC3 [35]. In our research, we also illustrated that the levels of HDAC3 expression remained largely unchanged in TGFβ-treated RPE cells; however, HDAC3 was significantly upregulated in EGF-induced EMT in human RPE cells. It was thought-provoking that the upregulation of HDAC3 was mediated by EGF rather than TGFβ. Here, we further found that HDAC3 inhibition limited the EMT phenotype in RPE cells. It should be mentioned that alpha-SMA is a marker of myofibroblasts, which is upregulated in fibrosis diseases [36,37]. EGF stimulation resulted in a notable decrease in the expression of E-Cadherin and a concurrent increase in the expression of alpha-SMA. Our findings showed that HDAC3 inhibition reversed the EGF-induced expression of EMT-related molecules in RPE cells. Additionally, we found that HDAC3 overexpression upregulated alpha-SMA expression and downregulated E-Cadherin expression. Thus, it was speculated that HDAC3 may be recognized as a target to abrogate the EMT phenotype in RPE cells.

The migration of RPE cells is strongly linked to the onset of PVR [32]. During the PVR progression, RPE cells disengage from

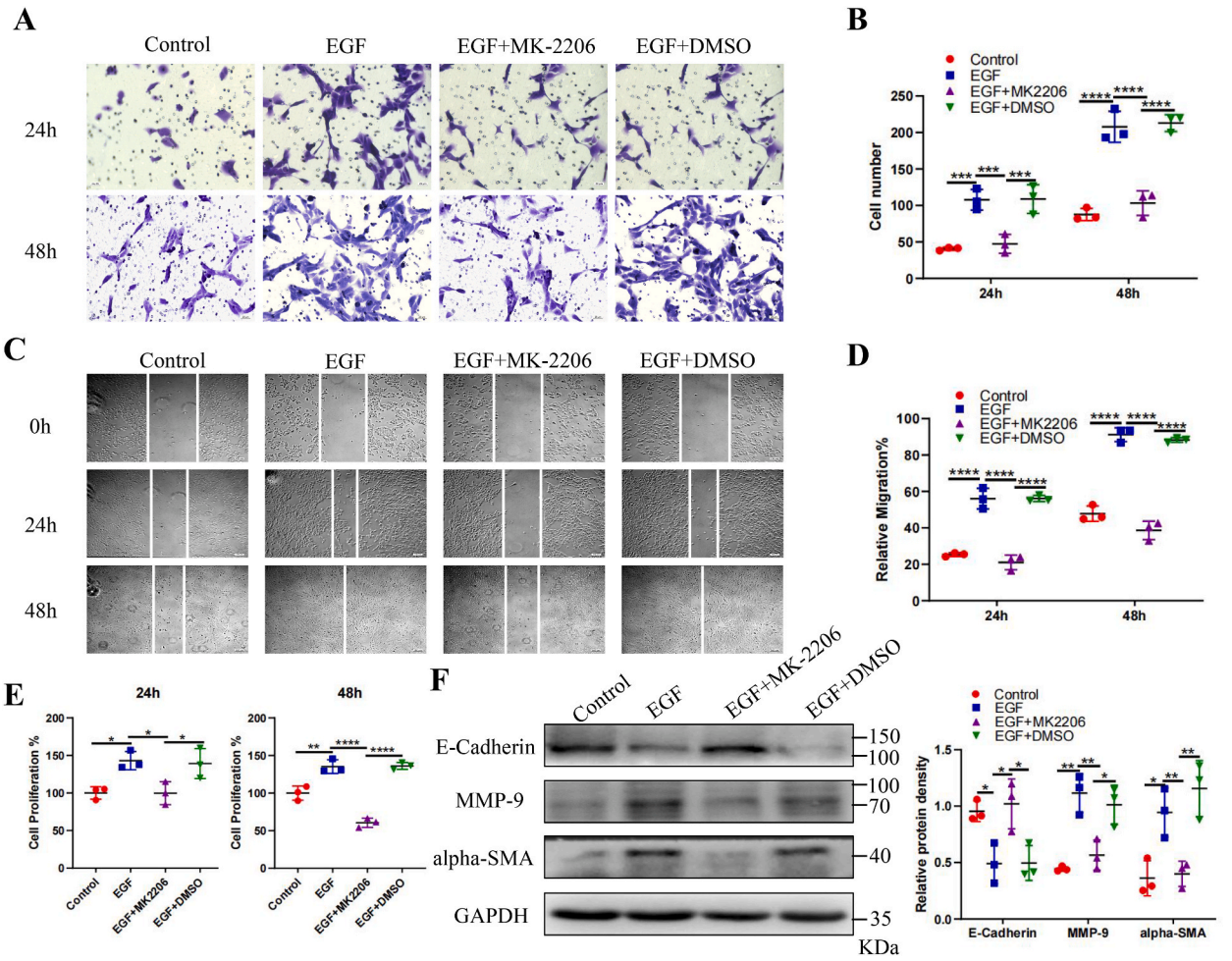

Fig. 8. The AKT pathway played a crucial role in the EMT model induced by EGF in ARPE-19 cells. (A)The transwell assay was used to detect the migration of ARPE-19 cells following treatment with MK2206 or DMSO. Scale bar, 25 μm; n = 3. (B)The statistical analysis of the data presented in Fig. 8A demonstrated the significant decrease in EGF-induced cell migration by MK-2206 at both 24 and 48-h time points. ***$P < 0.001$; ****$P < 0.0001$; n = 3. (C)The scratch assay was used to examine ARPE-19 cells' wound-repair abilities. Scale bar, 100 μm; n = 3. (D)The quantitative assessment of the rate of wound closure. ****$P < 0.0001$; n = 3. (E)ARPE-19 cells were exposed to a combination of 20 ng/ml EGF and 10 μM MK-2206 for 24 h or 48 h. Cell proliferation was evaluated using the CCK-8 assay. *$P < 0.05$; **$P < 0.01$; ****$P < 0.0001$; n = 3. (F)Western blot assay was conducted to analyze the levels of E-Cadherin, MMP-9, and alpha-SMA expression in APRE-19 cells treatment with MK-2206 or DMSO and exposure to EGF. *$P < 0.05$; **$P < 0.01$; n = 3.

Bruch's membrane and move towards the vitreous cavity to establish the proliferative membranes [32,38]. In the present study, the inhibition of HDAC3 notably suppressed the EGF-induced RPE cell migration, as demonstrated by both transwell assay and scratch assay. During the migration process, RPE cells secreted various matrix metalloproteinases(MMPs) that broke down the basement membrane and produced a great quantity of extracellular matrix(ECM), such as collagen. Among the family of MMPs, MMP-9 appears to exhibit the strongest association with cell migration [39]. Our findings showed that the level of MMP-9 expression was upregulated in RPE cells during the EMT process, and the elevated level could be downregulated by HDAC3 inhibition. Based on these data, we speculated that HDAC3 inhibition suppressed the migration of RPE cells treated with EGF partly attributing to the downregulation of MMP-9.

To further investigate the expression of HDAC3 in EGF-treated ARPE-19 cells, we conducted an examination of the transcription factors associated with HDAC3 expression. Our findings revealed that MAZ, a Myc-associated zinc-finger protein, directly interacted with the HDAC3 promoter region and stimulated its expression. As an important transcription factor, MAZ has been observed to be highly expressed in diverse human cancer types, which was implicated in the EMT process of tumor cells [40–42]. In hepatocellular carcinoma, a study from Wei et al. has reported that MAZ promoted the invasion and metastasis of hepatocellular carcinoma by inducing EMT through upregulating the expression of ZEB1 and ZEB2 [41]. In addition, a recent study revealed that MAZ promoted the progression of breast cancer by regulating SIPL1 [43]. These studies indicated that MAZ facilitated cancer cell metastasis and EMT by the modulation of the downstream target genes. In our study, it was observed that the level of MAZ was elevated in human PVR

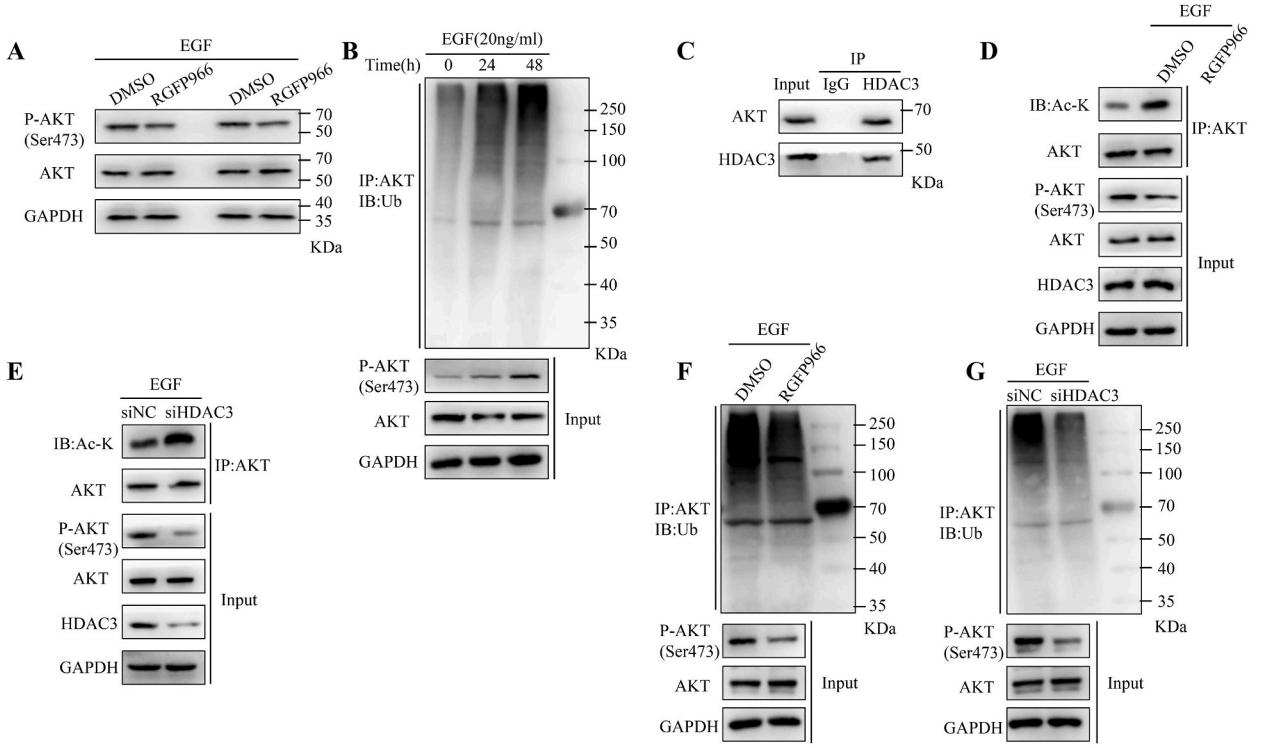

Fig. 9. HDAC3 promoted the phosphorylation of AKT by deacetylating AKT. (A)ARPE-19 cells were exposed to 20 μM of CHX for 12 h, after which they were subjected to treatment with RGFP966(15 μM) for 48 h for subsequent Western blot analysis using specified antibodies. n = 3. (B) ARPE-19 cells were exposed to a concentration of 20 ng/ml of EGF for varying durations, followed by a collection for IP and Western blot analysis using specified antibodies. (C)The relationship between HDAC3 and AKT was analyzed by Co-IP. (D)RGFP966 was used to inhibit HDAC3. The acetylation of AKT was investigated by IP. (E)HDAC3-siRNA was used to knock down the expression of HDAC3. The acetylation of AKT was tested by IP. (F)RGFP966 was used to inhibit HDAC3. The polyubiquitination of AKT was detected by IP. (G)HDAC3-siRNA was used to knock down the expression of HDAC3. The polyubiquitination of AKT was determined by IP.

membranes and EGF-induced EMT of RPE cells. Additionally, it was found that MAZ facilitated the transcriptional expression of HDAC3, suggesting a potentially significant involvement of MAZ in the EMT process of RPE cells. Further research is necessary to elucidate the mechanisms through which MAZ influences the EMT of RPE cells.

The AKT kinase also referred to as protein kinase B, is significantly involved in cell proliferation, growth, apoptosis, and metabolism [44], which has been proven to play a key role in the EMT of RPE cells [45–47]. Activation of AKT occurs through phosphorylation at Thr308 and subsequent phosphorylation at Ser473 in response to various growth factors such as EGF [48,49]. Our study also indicated that EGF led to an increase in AKT phosphorylation in RPE cells, and AKT inhibitor MK-2206 attenuated EGF-induced EMT of RPE cells, suggesting that AKT played a vital role in RPE-EMT. Besides phosphorylation, other post-translational modifications are also important in regulating the activity of AKT, including polyubiquitination and acetylation [50]. It was reported that the inhibitors of class I/II HDACs could suppress the phosphorylation of AKT by Chen et al. [51]. In agreement with the research, our results indicated that HDAC3 inhibition downregulated EGF-induced AKT phosphorylation. One possible explanation for this result was that the inhibitor potentially affected the production of upstream regulators, such as PHLPP1, a protein known to decrease the phosphorylation of AKT [52]. However, our findings provided evidence that CHX treatment had only a negligible impact on the inhibition of AKT phosphorylation induced by RGFP966, indicating that RGFP966's lowered AKT phosphorylation was not largely facilitated by its influence on the expression of AKT upstream regulators. Our experiments further confirmed that HDAC3 interacted with AKT, promoting the polyubiquitination of AKT by deacetylating it, which ultimately led to AKT phosphorylation and activity. Consistent with our study, the relationship between HDAC3 and AKT has also been observed in PTEN- or SPOP-mutated prostate cancer [53].

In this study, our results demonstrated for the first time the significant involvement of HDAC3 in the EMT of RPE cells during the formation of PVR by upregulating the phosphorylation of AKT. Inhibiting HDAC3 in RPE cells can impede EMT and slow the evolution of PVR. Given the close association between EMT of RPE cells and PVR, these findings offer new insights into the pathogenesis of PVR and suggest a possible therapeutic target for its prevention and therapy.

5. Conclusions

Our results indicate that HDAC3 is the key determinant of PVR development and EMT of RPE cells, and suggest that HDAC3 could

serve as a promising therapeutic target for the prevention and treatment of PVR.

Availability of data and materials

The data that support the findings of this study are openly available to other researchers upon reasonable request.

CRediT authorship contribution statement

Weikang Zou: Writing – original draft, Methodology, Data curation. **Chunling Huang:** Writing – original draft, Methodology, Data curation. **Yuting Chen:** Writing – original draft, Data curation. **Jing Tang:** Writing – original draft, Data curation. **Qiqi Li:** Methodology. **Qi Fang:** Methodology. **Yulin Ma:** Methodology. **Wei Wu:** Writing – review & editing, Funding acquisition. **Songfu Feng:** Writing – review & editing, Funding acquisition.

Ethics approval and consent to participate

Not applicable.

Consent for publication

Not applicable.

Funding

This study was supported by the Guangzhou Municipal Science and Technology Program(Grant No. 202002020046), the Western Medicine Project of Guangzhou Health Committee(Grant No. 20211A011022), and the Presidential Foundation of the Zhujiang Hospital of Southern Medical University(Grant No. yzjj2023ms19).

Declaration of competing interest

The authors declare that they have no known competing financial interests or personal relationships that could have appeared to influence the work reported in this paper.

Acknowledgments

Not applicable.

Abbreviations

PVR	**Proliferative vitreoretinopathy**
EMT	**Epithelial-mesenchymal transition**
RPE	**Retinal pigment epithelium**
HDAC3	Histone deacetylase3
GEO	Gene expression omnibus
EGF	Epidermal growth factor
ChIP	**Chromatin immunoprecipitation**
AKT	**Protein kinase B**
Alpha-SMA	Alpha-smooth muscle actin
APRE-19	Human retinal pigment epithelial cell line
DMEM	Dulbecco's modified Eagle's medium
FBS	Fetal bovine serum
CCK-8	Cell Counting Kit-8
SDS-PAGE	Sulfate-polyacrylamide gel electrophoresis
PVDF	Polyvinylidene difluoride
GAPDH	Glyceraldehyde 3-phosphate dehydrogenase
MAZ	Myc-associated zinc finger protein
TGF-β1	Transforming growth factor-beta 1
CHX	Cycloheximide

Appendix A. Supplementary data

Supplementary data to this article can be found online at https://doi.org/10.1016/j.heliyon.2024.e39333.

References

[1] S. Idrees, J. Sridhar, A.E. Kuriyan, Proliferative vitreoretinopathy: a review, Int. Ophthalmol. Clin. 59 (2019) 221–240.
[2] H.S. Mudhar, A brief review of the histopathology of proliferative vitreoretinopathy (PVR), Eye (Lond) 34 (2020) 246–250.
[3] C. Chiquet, F. Rouberol, [Proliferative vitreoretinopathy: prophylactic treatment], J FR OPHTALMOL 37 (2014) 737–743.
[4] F. Wu, D. Eliott, Molecular targets for proliferative vitreoretinopathy, Semin. Ophthalmol. 36 (2021) 218–223.
[5] W. Zhang, J. Li, EGF receptor signaling modulates YAP activation and promotes experimental proliferative vitreoretinopathy, Invest. Ophthalmol. Vis. Sci. 63 (2022) 24.
[6] H. Han, N. Chen, X. Huang, B. Liu, J. Tian, H. Lei, Phosphoinositide 3-kinase δ inactivation prevents vitreous-induced activation of AKT/MDM2/p53 and migration of retinal pigment epithelial cells, J. Biol. Chem. 294 (2019) 15408–15417.
[7] X. Ma, S. Han, Y. Liu, Y. Chen, P. Li, X. Liu, L. Chang, Y.A. Chen, F. Chen, Q. Hou, L. Hou, DAPL1 prevents epithelial-mesenchymal transition in the retinal pigment epithelium and experimental proliferative vitreoretinopathy, Cell Death Dis. 14 (2023) 158.
[8] X. Ma, Y. Xie, Y. Gong, C. Hu, K. Qiu, Y. Yang, H. Shen, X. Zhou, C. Long, X. Lin, Silibinin prevents tgfβ-induced EMT of RPE in proliferative vitreoretinopathy by inhibiting Stat3 and Smad3 phosphorylation, Invest. Ophthalmol. Vis. Sci. 64 (2023) 47.
[9] D. Li, D. Yuan, H. Shen, X. Mao, S. Yuan, Q. Liu, Gremlin-1: an endogenous BMP antagonist induces epithelial-mesenchymal transition and interferes with redifferentiation in fetal RPE cells with repeated wounds, Mol. Vis. 25 (2019) 625–635.
[10] S. Yang, H. Li, M. Li, F. Wang, Mechanisms of epithelial-mesenchymal transition in proliferative vitreoretinopathy, Discov. Med. 20 (2015) 207–217.
[11] X. Ma, C. Long, F. Wang, B. Lou, M. Yuan, F. Duan, Y. Yang, J. Li, X. Qian, J. Zeng, S. Lin, H. Shen, X. Lin, METTL3 attenuates proliferative vitreoretinopathy and epithelial-mesenchymal transition of retinal pigment epithelial cells via wnt/β-catenin pathway, J. Cell Mol. Med. 25 (2021) 4220–4234.
[12] S. He, E. Barron, K. Ishikawa, K.H. Nazari, C. Spee, P. Zhou, S. Kase, Z. Wang, L.D. Dustin, D.R. Hinton, Inhibition of DNA methylation and methyl-CpG-binding protein 2 suppresses RPE transdifferentiation: relevance to proliferative vitreoretinopathy, Invest. Ophthalmol. Vis. Sci. 56 (2015) 5579–5589.
[13] Y.T. Lin, K.J. Wu, Epigenetic regulation of epithelial-mesenchymal transition: focusing on hypoxia and TGF-β signaling, J. Biomed. Sci. 27 (2020) 39.
[14] M. Edderkaoui, C. Chheda, B. Soufi, F. Zayou, R.W. Hu, V.K. Ramanujan, X. Pan, L.G. Boros, J. Tajbakhsh, A. Madhav, N.A. Bhowmick, Q. Wang, M. Lewis, R. Tuli, A. Habtezion, R. Murali, S.J. Pandol, An inhibitor of GSK3B and HDACs kills pancreatic cancer cells and slows pancreatic tumor growth and metastasis in mice, Gastroenterology 155 (2018) 1985–1998.e5.
[15] X.T. Hu, W. Xing, R.S. Zhao, Y. Tan, X.F. Wu, L.Q. Ao, Z. Li, M.W. Yao, M. Yuan, W. Guo, S.Z. Li, J. Yu, X. Ao, X. Xu, HDAC2 inhibits EMT-mediated cancer metastasis by downregulating the long noncoding RNA H19 in colorectal cancer, J. Exp. Clin. Cancer Res. 39 (2020) 270.
[16] S.H. Jeong, E.S. Son, Y.E. Lee, S.Y. Kyung, J.W. Park, S.H. Kim, Histone deacetylase 3 promotes alveolar epithelial-mesenchymal transition and fibroblast migration under hypoxic conditions, Exp. Mol. Med. 54 (2022) 922–931.
[17] R. He, B. Liu, B. Geng, N. Li, Q. Geng, The role of HDAC3 and its inhibitors in regulation of oxidative stress and chronic diseases, Cell Death Dis. 9 (2023) 131.
[18] S.M. Wu, Y.J. Jan, S.C. Tsai, H.C. Pan, C.C. Shen, C.N. Yang, S.H. Lee, S.H. Liu, L.W. Shen, C.S. Chiu, J.L. Arbiser, M. Meng, M.L. Sheu, Targeting histone deacetylase-3 blocked epithelial-mesenchymal plasticity and metastatic dissemination in gastric cancer, Cell Biol. Toxicol. 39 (2023) 1873–1896.
[19] R. Xiong, B. Geng, W. Jiang, Y. Hu, Z. Hu, B. Hao, N. Li, Q. Geng, Histone deacetylase 3 deletion in alveolar type 2 epithelial cells prevents bleomycin-induced pulmonary fibrosis, CLIN EPIGENETICS 15 (2023) 182.
[20] L. Zhang, X. Shan, Q. Chen, D. Xu, X. Fan, M. Yu, Q. Yan, J. Liu, Downregulation of HDAC3 by ginsenoside Rg3 inhibits epithelial-mesenchymal transition of cutaneous squamous cell carcinoma through c-Jun acetylation, J. Cell. Physiol. 234 (2019) 22207–22219.
[21] S.H. Chen, Y.J. Lin, L.C. Wang, H.Y. Tsai, C.H. Yang, Y.T. Teng, S.M. Hsu, Doxycycline ameliorates the severity of experimental proliferative vitreoretinopathy in mice, Int. J. Mol. Sci. 22 (2021).
[22] E.A. Abu, L. Missotten, K. Geboes, Expression of myofibroblast activation molecules in proliferative vitreoretinopathy epiretinal membranes, Acta Ophthalmol. 89 (2011) e115–e121.
[23] S. Piera-Velazquez, Z. Li, S.A. Jimenez, Role of endothelial-mesenchymal transition (EndoMT) in the pathogenesis of fibrotic disorders, Am. J. Pathol. 179 (2011) 1074–1080.
[24] F. Yan, Y.N. Hui, Y.J. Li, C.M. Guo, H. Meng, Epidermal growth factor receptor in cultured human retinal pigment epithelial cells, Ophthalmologica 221 (2007) 244–250.
[25] C. Baudouin, D. Fredj-Reygrobellet, F. Brignole, F. Nègre, P. Lapalus, P. Gastaud, Growth factors in vitreous and subretinal fluid cells from patients with proliferative vitreoretinopathy, Ophthalmic Res. 25 (1993) 52–59.
[26] Y. Shao, J. Chen, J. Zheng, C.R. Liu, Effect of histone deacetylase HDAC3 on cytokines IL-18, IL-12 and TNF-α in patients with intrahepatic cholestasis of pregnancy, Cell. Physiol. Biochem. 42 (2017) 1294–1302.
[27] L. Chen, C. Shang, B. Wang, G. Wang, Z. Jin, F. Yao, Z. Yue, L. Bai, R. Wang, S. Zhao, E. Liu, W. Wang, HDAC3 inhibitor suppresses endothelial-to-mesenchymal transition via modulating inflammatory response in atherosclerosis, Biochem. Pharmacol. 192 (2021) 114716.
[28] V. Pooladanda, S. Thatikonda, S. Bale, B. Pattnaik, D.K. Sigalapalli, N.B. Bathini, S.B. Singh, C. Godugu, Nimbolide protects against endotoxin-induced acute respiratory distress syndrome by inhibiting TNF-α mediated NF-κB and HDAC-3 nuclear translocation, Cell Death Dis. 10 (2019) 81.
[29] W.L. Yang, J. Wang, C.H. Chan, S.W. Lee, A.D. Campos, B. Lamothe, L. Hur, B.C. Grabiner, X. Lin, B.G. Darnay, H.K. Lin, The E3 ligase TRAF6 regulates Akt ubiquitination and activation, SCIENCE 325 (2009) 1134–1138.
[30] X.J. Yang, E. Seto, Lysine acetylation: codified crosstalk with other posttranslational modifications, MOL CELL 31 (2008) 449–461.
[31] K. Umazume, Y. Barak, K. McDonald, L. Liu, H.J. Kaplan, S. Tamiya, Proliferative vitreoretinopathy in the Swine-a new model, Invest. Ophthalmol. Vis. Sci. 53 (2012) 4910–4916.
[32] R.J. Feist, J.L. King, R. Morris, C.D. Witherspoon, C. Guidry, Myofibroblast and extracellular matrix origins in proliferative vitreoretinopathy, Graefes Arch. Clin. Exp. Ophthalmol. 252 (2014) 347–357.
[33] P. Karagianni, J. Wong, HDAC3: taking the SMRT-N-CoRrect road to repression, Oncogene 26 (2007) 5439–5449.
[34] Z. Chen, L. Pei, D. Zhang, F. Xu, E. Zhou, X. Chen, HDAC3 increases HMGB3 expression to facilitate the immune escape of breast cancer cells via down-regulating microRNA-130a-3p, Int. J. Biochem. Cell Biol. 135 (2021) 105967.
[35] W. Xiao, X. Chen, X. Liu, L. Luo, S. Ye, Y. Liu, A. Trichostatin, A histone deacetylase inhibitor, suppresses proliferation and epithelial-mesenchymal transition in retinal pigment epithelium cells, J. Cell Mol. Med. 18 (2014) 646–655.
[36] S. Lamouille, J. Xu, R. Derynck, Molecular mechanisms of epithelial-mesenchymal transition, Nat. Rev. Mol. Cell Biol. 15 (2014) 178–196.
[37] A. Dongre, R.A. Weinberg, New insights into the mechanisms of epithelial-mesenchymal transition and implications for cancer, Nat. Rev. Mol. Cell Biol. 20 (2019) 69–84.
[38] H. Zou, C. Shan, L. Ma, J. Liu, N. Yang, J. Zhao, Polarity and epithelial-mesenchymal transition of retinal pigment epithelial cells in proliferative vitreoretinopathy, PeerJ 8 (2020) e10136.
[39] S.A. Ozal, V. Gurlu, K. Turkekul, H. Guclu, S. Erdogan, Neferine inhibits epidermal growth factor-induced proliferation and migration of retinal pigment epithelial cells through downregulating p38 MAPK and PI3K/AKT signalling, Cutan. Ocul. Toxicol. 39 (2020) 97–105.
[40] Y. Wang, L. Sun, W. Qiu, W. Qi, Y. Qi, Z. Liu, S. Liu, J. Lv, Inhibiting Forkhead box K1 induces autophagy to reverse epithelial-mesenchymal transition and metastasis in gastric cancer by regulating Myc-associated zinc finger protein in an acidic microenvironment, Aging (Albany NY) 12 (2020) 6129–6150.
[41] W. Luo, X. Zhu, W. Liu, Y. Ren, C. Bei, L. Qin, X. Miao, F. Tang, G. Tang, S. Tan, MYC associated zinc finger protein promotes the invasion and metastasis of hepatocellular carcinoma by inducing epithelial mesenchymal transition, Oncotarget 7 (2016) 86420–86432.
[42] C. Zheng, H. Wu, S. Zhang, R. Tian, H. Long, H. Zhang, X. Guo, D. Li, S. Tan, X. Zhu, Myc-associated zinc finger protein promotes metastasis of papillary thyroid cancer, Front Biosci (Landmark Ed) 28 (2023) 162.
[43] J. He, J. Wang, T. Li, K. Chen, S. Li, S. Zhang, SIPL1, regulated by MAZ, promotes tumor progression and predicts poor survival in human triple-negative breast cancer, FRONT ONCOL 11 (2021) 766790.

[44] M. Song, A.M. Bode, Z. Dong, M.H. Lee, AKT as a therapeutic target for cancer, Cancer Res. 79 (2019) 1019–1031.
[45] A.R. Learte, M.G. Forero, A. Hidalgo, Gliatrophic and gliatropic roles of PVF/PVR signaling during axon guidance, Glia 56 (2008) 164–176.
[46] L. Dong, H. Han, X. Huang, G. Ma, D. Fang, H. Qi, Z. Han, L. Wang, J. Tian, B. Vanhaesebroeck, G. Zhang, S. Zhang, H. Lei, Idelalisib inhibits experimental proliferative vitroretinopathy, Lab. Invest. 102 (2022) 1296–1303.
[47] H. Chen, H. Wang, J. An, Q. Shang, J. Ma, Plumbagin induces RPE cell cycle arrest and apoptosis via p38 MARK and PI3K/AKT/mTOR signaling pathways in PVR, BMC Complement Altern Med 18 (2018) 89.
[48] I.H. Yang, Y.T. Tsai, S.J. Chiu, L.T. Liu, H.H. Lee, M.F. Hou, W.L. Hsu, B.K. Chen, W.C. Chang, Involvement of STIM1 and Orai1 in EGF-mediated cell growth in retinal pigment epithelial cells, J. Biomed. Sci. 20 (2013) 41.
[49] S.F. Yang, Y.S. Chen, H.W. Chien, K. Wang, C.L. Lin, H.L. Chiou, C.Y. Lee, P.N. Chen, Y.H. Hsieh, Melatonin attenuates epidermal growth factor-induced cathepsin S expression in ARPE-19 cells: implications for proliferative vitreoretinopathy, J. Pineal Res. 68 (2020) e12615.
[50] H. Hua, H. Zhang, J. Chen, J. Wang, J. Liu, Y. Jiang, Targeting Akt in cancer for precision therapy, J. Hematol. Oncol. 14 (2021) 128.
[51] C.S. Chen, S.C. Weng, P.H. Tseng, H.P. Lin, C.S. Chen, Histone acetylation-independent effect of histone deacetylase inhibitors on Akt through the reshuffling of protein phosphatase 1 complexes, J. Biol. Chem. 280 (2005) 38879–38887.
[52] E.W. Bradley, L.R. Carpio, J.J. Westendorf, Histone deacetylase 3 suppression increases PH domain and leucine-rich repeat phosphatase (Phlpp)1 expression in chondrocytes to suppress Akt signaling and matrix secretion, J. Biol. Chem. 288 (2013) 9572–9582.
[53] Y. Yan, J. An, Y. Yang, D. Wu, Y. Bai, W. Cao, L. Ma, J. Chen, Z. Yu, Y. He, X. Jin, Y. Pan, T. Ma, S. Wang, X. Hou, S.J. Weroha, R.J. Karnes, J. Zhang, J. J. Westendorf, L. Wang, Y. Chen, W. Xu, R. Zhu, D. Wang, H. Huang, Dual inhibition of AKT-mTOR and AR signaling by targeting HDAC3 in PTEN- or SPOP-mutated prostate cancer, EMBO Mol. Med. 10 (2018).